

# MAASS FORMS ON $GL(3)$ AND $GL(4)$

DAVID W. FARMER, SALLY KOUTSOLIOTAS, AND STEFAN LEMURELL

ABSTRACT. We describe a practical method for finding an  $L$ -function without first finding the associated underlying object. The procedure involves using the Euler product and the approximate functional equation in a new way. No use is made of the functional equation of twists of the  $L$ -function. The method is used to find a large number of Maass forms on  $SL(3, \mathbb{Z})$  and to give the first examples of Maass forms of higher level on  $GL(3)$ , and on  $GL(4)$  and  $Sp(4)$ .

## 1. INTRODUCTION

We describe a general approach to finding an  $L$ -function given only a limited amount of information about its functional equation and Euler product. We illustrate the method by locating  $L$ -functions associated to Maass forms on  $SL(3, \mathbb{Z})$  and some of its subgroups, and on  $Sp(4, \mathbb{Z})$  and  $SL(4, \mathbb{Z})$ .

**1.1. Summary of the method and results.** We describe an approach to solving the following problem: find all  $L$ -functions satisfying a given functional equation. The precise assumptions, which also involve an Euler product and a Ramanujan bound on the coefficients, are given in Section 3.1. Our results show that, at least for  $L$ -functions of degree  $d \leq 4$ , this problem can be solved in a practical way, without an assumption of a functional equation for twists of the  $L$ -function and without first finding an arithmetic object that gives rise to the  $L$ -function.

Our approach involves a new way of extracting information from the smoothed approximate functional equation for an  $L$ -function. This formula, given in Theorem 4.1, is a standard tool in analytic number theory. The new ingredient makes use of the fact that a variety of test functions can appear in the formula. This allows us to create a relatively small system of equations which the Dirichlet coefficients of the unknown  $L$ -function must satisfy. Solving that system provides the missing information about the  $L$ -functions with the given functional equation.

Using this method, we have found more than 2000  $L$ -functions of Maass forms on  $SL(3, \mathbb{Z})$  and several dozen  $L$ -functions of Maass forms on congruence subgroups of  $SL(3, \mathbb{Z})$ . The method also shows the non-existence of small eigenvalues for Maass forms on  $SL(3, \mathbb{Z})$  in a manner that is more effective than previous results using the explicit formula [20].

We have also found more than 200  $L$ -functions of Maass forms on  $SL(4, \mathbb{Z})$  and several dozen for  $Sp(4, \mathbb{Z})$ . The smallest  $Sp(4, \mathbb{Z})$  example has the surprising property that its first zero on the critical line has a larger imaginary part than the first zero of the Riemann zeta-function [3]. We have also used this method to find, with proof, the smallest conductor of a hyperelliptic curve [11].

---

The authors thank Ce Bian, Andrew Booker, Brian Conrey, Stephen D. Miller, Michael Rubinstein, Ralf Schmidt, and Nicolas Templier for helpful discussions.

Several independent tests are applied to our examples, and confirm our results in all cases. This gives us confidence to claim that our approximate functional equation method does indeed find  $L$ -functions without the need to first identify the underlying object.

Our data will be made available at <http://www.LMFDB.org/L/degree3> and [/degree4](http://www.LMFDB.org/L/degree4).

## 2. PRIOR METHODS

We describe methods which have been used to find automorphic forms on  $GL(2)$ , as well as recent approaches for higher rank groups.

**2.1. Holomorphic modular forms and Fourier series methods.** There are two types of modular forms on a Hecke congruence group  $\Gamma_0(N) \subset SL(2, \mathbb{Z})$ : holomorphic modular forms and Maass forms. Constructing holomorphic modular forms is relatively straightforward. If the level,  $N$ , is small, then one can find an explicit basis of the ring of modular forms on  $\Gamma_0(N)$ . For any level  $N$  and any weight  $k$ , one can use modular symbols [27] to produce a spanning set for the space  $S_k(\Gamma_0(N))$ . Diagonalizing with respect to the Hecke operators and the Atkin-Lehner operators gives the basis of newforms, which have algebraic integer Fourier coefficients. This process has been completely automated [24].

For Maass forms, the situation is quite different. Except for a thin set arising from quadratic fields, there is no known explicit construction of these functions. Thus, for most Maass forms one must rely on computer calculations to determine numerical approximations [12, 15, 28]. Recently, such computations have been proven to be correct [5].

The methods used to find Maass forms on  $GL(2)$  make use of the Fourier expansion and the transformation properties under elements of the group. For  $GL(d)$ ,  $d \geq 3$ , the Maass forms are functions of  $\frac{1}{2}(d^2 + d - 2)$  real variables. Their Fourier expansions [6, 14] are  $(d - 1)$ -fold sums over the integers, with an embedded sum over cosets of  $SL(d - 1, \mathbb{Z})$ . The complicated nature of the sum makes it difficult to directly find Maass forms on  $SL(3, \mathbb{Z})$ , although partial success has been reported by Bian and Mezhericher [1, 18]. For  $SL(4, \mathbb{Z})$  and higher, that approach is probably infeasible.

**2.2.  $L$ -function methods.** A natural alternative to dealing with the Maass form is to work directly with its  $L$ -function. There is no loss of information passing between those functions since the spectral data and Fourier coefficients of the Maass form can be recovered from the  $L$ -function. This approach was used successfully by Bian [1, 2], who made use of the functional equations for twists of the  $L$ -function, invoking the  $GL(3)$  converse theorem. The method involved solving a system of linear equations with approximately 10,000 unknowns. More details on Bian's method are given in Section 6. Another approach was suggested by Miller [19], based on the Voronoi summation formula.

In this paper we present an approach which also involves finding the  $L$ -function, but we assume only one functional equation and do not make the assumption of a functional equation for twists. Instead, we make use of the Euler product to produce additional relations. This approach enables us to work with a very small system of equations, typically fewer than 30 unknowns, although it is a non-linear system.

In the next section we describe the results we have obtained with our method, and in Section 4 we give details about our algorithm.

## 3. NOTATION AND RESULTS

There have been several axiomatic definitions of “ $L$ -function,” most notably that of Selberg [25] who conjectured that the functions in the Selberg class coincide with those arising from automorphic representations. Below, we give a more restrictive set of axioms, which describes the properties that are known or conjectured to hold for  $L$ -functions associated to a unitary cuspidal automorphic representation of  $GL(d)$ .

**3.1.  $L$ -function axioms.** We consider  $L$ -functions given by a Dirichlet series

$$L(s) = \sum_{n=1}^{\infty} \frac{a_n}{n^s}, \quad (3.1)$$

where  $a_n \ll n^\epsilon$  for any  $\epsilon > 0$ . The estimate on the Dirichlet coefficients is known as the *Ramanujan bound*.

The Ramanujan bound implies that the Dirichlet series (3.1) converges absolutely for  $\sigma = \Re(s) > 1$ . We assume that  $L(s)$  continues to an entire function. (In general an  $L$ -function can have a pole at  $s = 1$ , but the  $L$ -functions we consider will be entire.) We assume that the completed  $L$ -function,  $\Lambda(s)$ , is entire and bounded in vertical strips, and satisfies a functional equation of the form

$$\begin{aligned} \Lambda(s) &= N^{\frac{s}{2}} \prod_{j=1}^{d_1} \Gamma_{\mathbb{R}}(s + \mu_j) \prod_{j=1}^{d_2} \Gamma_{\mathbb{C}}(s + \nu_j) \cdot L(s) \\ &= \varepsilon \overline{\Lambda}(1 - s), \end{aligned} \quad (3.2)$$

where  $N$  is a positive integer called the *level*, and  $|\varepsilon| = 1$ . Here  $\Gamma_{\mathbb{R}}(s) = \pi^{-s/2} \Gamma(s/2)$  and  $\Gamma_{\mathbb{C}}(s) = 2(2\pi)^{-s} \Gamma(s)$  where  $\Gamma$  is the Euler  $\Gamma$ -function, and  $\overline{\Lambda}(z) = \overline{\Lambda(\bar{z})}$ . The integer  $d = d_1 + 2d_2$  is called the *degree* of the  $L$ -function. The analogue of the Selberg eigenvalue conjecture is that  $\Re(\mu_j), \Re(\nu_j) \geq 0$ .

We also assume an Euler product of the form

$$L(s) = \prod_{p|N} L_p(s) \prod_{p \nmid N} L_p(s), \quad (3.3)$$

where  $L_p(s) = f_p(p^{-s})^{-1}$  with  $f_p$  a polynomial with  $f_p(0) = 1$ . If  $p \nmid N$  then we assume  $f_p$  has degree  $d$  and satisfies the self-reciprocal condition  $f_p(z) = \chi(p)(-1)^d z^d \overline{f_p(z^{-1})}$ , where  $\chi$  is a Dirichlet character mod  $N$ , known as the *central character* of the  $L$ -function. If  $p|N$  then we assume  $f_p$  has degree  $\leq d - 1$ .

An equivalent formulation of the Ramanujan bound is that if  $p \nmid N$  then all roots of  $f_p$  lie on the unit circle, and if  $p|N$  then all roots of  $f_p$  lie on or outside the unit circle. This implies a more precise form of the Ramanujan bound:

$$|a(p^m)| \leq \binom{m + d - 1}{d - 1}. \quad (3.4)$$

**3.2.  $L$ -functions of Maass forms.** If  $F$  is a Maass form on  $SL(d, \mathbb{Z})$  with Fourier coefficients  $(a_{n_1, \dots, n_{d-1}})$ , then its  $L$ -function  $L(s, F)$  has Dirichlet coefficients  $a_n = a_{n_1, \dots, n_{d-1}}$ . The  $L$ -function has an Euler product of the form (3.3) with  $\omega_p = 1$ . The Ramanujan bound has not been proven in this case. The  $L$ -function satisfies a functional equation of the form (3.2) with  $N = 1$ ,  $\varepsilon = 1$ ,  $d_1 = d$ ,  $d_2 = 0$ , and  $\{\mu_1, \dots, \mu_{d-1}\} = \{i\lambda_1, \dots, i\lambda_{d-1}\}$ , where the  $\lambda_i$

have simple expressions in terms of the eigenvalues of the Maass form under the generators of the ring of invariant differential operators, and  $\mu_d = -\sum_{j < d} \mu_j$ . The Selberg eigenvalue conjecture asserts that the  $\lambda_j$  are real. This was proven by Miller [20] when  $N = 1$  and  $d = 3$ . See [6, 14] for more details about these  $L$ -functions.

**3.3. Results for  $SL(3, \mathbb{Z})$ .** We continue the notation of Section 3.2 with  $d = 3$ .

By permuting the  $\lambda_j$  and possibly replacing the  $L$ -function by its dual (conjugate), we can assume  $\lambda_1 \geq \lambda_2 \geq 0$  and  $\lambda_3 = -\lambda_1 - \lambda_2$ . Thus, we specify the functional equation of the  $L$ -function, equivalently the eigenvalues of the Maass form, by a point  $(\lambda_1, \lambda_2)$  below the diagonal of the first quadrant of  $\mathbb{R}^2$ . The symmetric squares of  $SL(2, \mathbb{Z})$  Maass forms have  $\lambda_2 = 0$ .

Weyl's law for  $SL(3, \mathbb{Z})$ , proved by Miller [20], asserts that

$$\#\{(\lambda_1, \lambda_2) : \lambda_1^2 + \lambda_1\lambda_2 + \lambda_2^2 \leq T\} \sim \frac{\text{vol}(X)}{(4\pi)^{\frac{5}{2}}\Gamma(\frac{7}{2})} T^{\frac{5}{2}}, \quad (3.5)$$

where  $X = SL(3, \mathbb{Z}) \backslash SL(3, \mathbb{R}) / SO(3, \mathbb{R})$ . Miller also proved the Selberg eigenvalue conjecture for  $SL(3, \mathbb{Z})$  in the form  $\lambda_1^2 + \lambda_1\lambda_2 + \lambda_2^2 \geq 80$ . (Miller proved slightly more, which is described in Figure 3.1 below.)

The purpose of this paper is to describe a new method for finding  $L$ -functions satisfying the axioms given in Section 3.1. Our results fall into two categories: an extension of Miller's result that certain regions do not contain the eigenvalues of any  $SL(3, \mathbb{Z})$  Maass forms, and the experimental determination of a large number of  $L$ -functions that appear to arise from  $SL(3, \mathbb{Z})$  Maass forms. Both types of results are displayed in Figure 3.1.

The dark-shaded region in Figure 3.1 was shown by Miller [20], using the explicit formula, to contain no eigenvalues  $(\lambda_1, \lambda_2)$  of any  $SL(3, \mathbb{Z})$  Maass forms. We use the approximate functional equation to prove a stronger result.

**Theorem 3.1.** *Assume the Ramanujan bound  $|a_p| \leq 3$ . There are no  $L$ -functions with functional equation (3.2) with  $d = 3$  and  $N = 1$ , therefore no  $SL(3, \mathbb{Z})$  Maass forms, with spectral parameters  $(\lambda_1, \lambda_2)$  in the lightly shaded region shown in Figure 3.1.*

The proof, which is a new application of the approximate functional equation, is given in Section 7.

Also shown in Figure 3.1 are the 124 lowest (in lexicographical order) pairs  $(\lambda_1, \lambda_2)$  of  $L$ -functions with functional equation and Euler product as described in Section 3.2 with  $d = 3$ , which were found in our search. We believe that the figure shows all cases with  $\lambda_1 \leq 20$ , and may include all with  $\lambda_1 \leq 24$ . Numerical values for the first 15 examples, and their first two Dirichlet coefficients, are listed in Table 3.1.

Ce Bian (personal communication) has confirmed several dozen of our examples and computed a few thousand Dirichlet coefficients in each of those cases.

We have found more than 2000 spectral parameters  $(\lambda_1, \lambda_2)$  and associated Dirichlet coefficients. These will be made available at <http://www.LMFDB.org/L/degree3>.

**3.4. Subgroups of  $SL(3, \mathbb{Z})$ .** We applied the approximate functional equation method to find  $L$ -functions associated to Maass forms on subgroups of  $SL(3, \mathbb{Z})$ . In terms of the functional equation, we have  $d_1 = 3$ ,  $d_2 = 0$ , and  $N > 1$ . For  $p|N$ , the local factor in the Euler product (3.3) will have degree at most 2. In our calculations, we assume an arbitrary degree-2 local factor at the primes dividing the level:  $L_p(s) = (1 + A_p p^{-s} + B_p p^{-2s})^{-1}$ . It

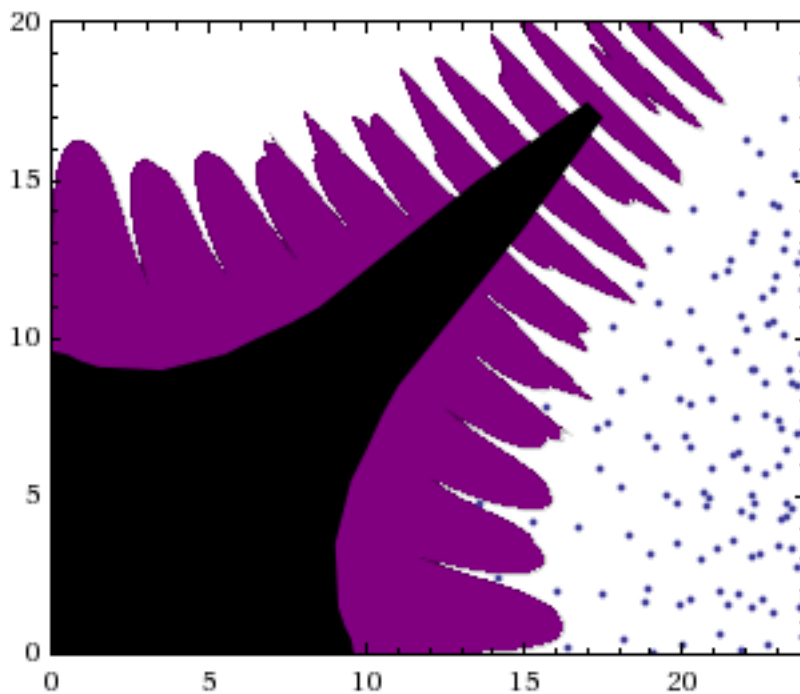


FIGURE 3.1. The axes are  $\lambda_1$  and  $\lambda_2$  and the dots indicate  $(\lambda_1, \lambda_2)$  for the parameters in the functional equation of  $SL(3, \mathbb{Z})$   $L$ -functions, for the first few examples we found. The darkest region is Miller's excluded region [20], and we prove, assuming the Ramanujan conjecture, that the lighter shaded region contains no eigenvalues.

| $\lambda_1$ | $\lambda_2$ | $a_2$                       | $a_3$                       |
|-------------|-------------|-----------------------------|-----------------------------|
| 13.59658451 | 4.76468206  | $1.04846245 - 0.37523963i$  | $-0.49904094 - 0.27897508i$ |
| 14.14163558 | 2.38038848  | $-0.10524097 + 0.75072694i$ | $1.23599391 - 0.03911217i$  |
| 15.31863407 | 4.19173391  | $0.33541208 + 0.34590083i$  | $-0.27260607 - 0.97283444i$ |
| 15.74069912 | 7.85232504  | $-0.39016397 - 0.62517821i$ | $0.75666087 - 0.16479552i$  |
| 16.05436164 | 1.98365457  | $-0.85221921 + 0.41800410i$ | $0.67428665 - 0.33153749i$  |
| 16.40312474 | 0.17112189  | $-0.42168648 + 1.06796797i$ | $-0.76802216 - 1.31329241i$ |
| 16.75957309 | 4.03941275  | $0.43484942 - 0.64408778i$  | $0.67804925 - 0.27020173i$  |
| 17.34401833 | 7.13419625  | $0.55207716 - 0.70388045i$  | $0.03833728 + 0.25697818i$  |
| 17.42523780 | 5.86543671  | $-0.86407728 - 1.64923555i$ | $-0.22106187 - 0.90868355i$ |
| 17.50092882 | 1.90552951  | $-0.28445287 + 0.01165958i$ | $0.42424909 + 0.46219014i$  |
| 17.65047391 | 7.30146768  | $-0.70569544 + 0.37307990i$ | $-0.29251139 + 1.07644911i$ |
| 17.86523805 | 10.34945597 | $-0.86106525 + 0.35416339i$ | $-0.13894817 + 0.24569291i$ |
| 18.06174615 | 8.34053395  | $-1.15143879 - 1.75641008i$ | $-0.49129679 + 0.21151351i$ |
| 18.08927092 | 5.30177649  | $0.32185117 + 0.32366378i$  | $-0.36219655 - 0.00596403i$ |
| 18.19481530 | 0.49254810  | $-1.15442278 + 1.90981460i$ | $0.33665482 - 0.10748733i$  |

TABLE 3.1. Spectral parameters  $(\lambda_1, \lambda_2)$  and sample Dirichlet series coefficients for the first 15  $L$ -functions of  $SL(3, \mathbb{Z})$  Maass forms. The numbers are truncated to 8 correct decimals.

may happen that  $B_p$  and/or  $A_p$  is zero, if the local factor had degree 0 or 1. By making no assumptions on the local factors, we have the opportunity for an independent check on our calculations.

We applied the approximate functional equation method to search for  $L$ -functions of levels  $N = 2$  and  $3$ , and trivial central character, and our search found nothing. This seemed at first to be problematic because when doing numerical experiments it can be difficult to distinguish a true non-result from a non-result due to a error in the computer program. In this particular case, it turns out that we experimentally discovered the theorem, which is relatively straightforward but does not seem to be in the literature: there are no Maass forms on  $GL(3)$  which give rise to  $L$ -functions of squarefree level and trivial central character. The most natural small index subgroups of  $SL(3, \mathbb{Z})$  have outer automorphisms (analogous to the Fricke involution for  $\Gamma_0(N)$ ) which give level  $p^2$  in the functional equation.

So we searched for  $L$ -functions of levels  $N = 4$ , and  $9$  and found examples in each case. For square level, the corresponding subgroups have outer automorphisms of order  $3$ . Therefore, the signs which appear in the functional equation should be  $3$ rd roots of  $1$ , and we found examples of all three signs. For level  $p^2$ , in every case the local factor we found at  $p$  was  $L_p(s) = (1 - \bar{\varepsilon}p^{-1-s})^{-1}$ , where  $\varepsilon$  is the sign of the functional equation. Note that we assumed a completely general degree  $2$  local factor, but then found that it actually had degree  $1$ .

Ralf Schmidt (personal communication) informed us that this is the local factor from the Steinberg representation for  $GL(3)$ , which has level  $p^2$ . This is a strong independent check of the validity of our calculations.

The first few  $L$ -functions for level  $4$  are given in Table 3.2. The expected lifts from  $GL(2)$  were found in our search.

**3.5. Results for  $Sp(4, \mathbb{Z})$  and  $GL(4, \mathbb{Z})$ .** We have also used our method to find degree  $4$   $L$ -functions, that is,  $L$ -functions with functional equation (3.2) and Euler product (3.3) with  $d = 4$ . At present, we consider the case of level  $N = 1$ ; we will address the situation of higher level in a subsequent paper.

It is natural to distinguish the special case where  $\lambda_1 = -\lambda_3$  and  $\lambda_2 = -\lambda_4$ , and the Dirichlet coefficients  $a_n$  are real. We refer to these as “ $Sp(4, \mathbb{Z})$   $L$ -functions” because we believe they are the spin  $L$ -functions of the analogue of Maass forms on  $Sp(4, \mathbb{Z})$ . Since the functional equation depends on two real parameters, we can provide a plot of our results, analogous to the case of  $SL(3, \mathbb{Z})$ . Figure 3.2 shows the first 58 examples that we have found for  $Sp(4, \mathbb{Z})$  Maass form  $L$ -functions. The first 15 of these are also listed in Table 3.3 with spectral parameters and the first four prime coefficients.

In Figure 3.2 one observes that the some of the first few  $L$ -functions lie approximately along certain lines. A similar phenomenon can be seen in Figure 3.1.

The first  $Sp(4, \mathbb{Z})$   $L$ -function, which has  $(\lambda_1, \lambda_2) = (12.46875, 4.72095)$  has the curious property that its lowest zero on the critical line is at  $\frac{1}{2} \pm 14.496i$ , which is higher than the lowest zero of the Riemann zeta-function. This is discussed further by Bober, et al. [3]. As a check on these calculations, we also compute the standard (degree  $5$ )  $L$ -function using the data from the spin (degree  $4$ )  $L$ -function (see section 6).

| $\epsilon$       | $\lambda_1$ | $\lambda_2$ | $a_2$                       | $a_3$                       |
|------------------|-------------|-------------|-----------------------------|-----------------------------|
| 1                | 8.23979752  | 2.64122672  | $1/2 + \delta$              | $1.06604225 + 0.48105885i$  |
| 1                | 10.64614640 | 5.40948610  | $1/2 + \delta$              | $0.06047305 - 0.43014710i$  |
| 1                | 11.72327411 | 2.02460527  | $1/2 + \delta$              | $0.59406181 - 0.27550311i$  |
| 1                | 12.42065536 | 4.72210152  | $1/2 + \delta$              | $0.99900525 - 0.54164255i$  |
| $e(\frac{1}{3})$ | 9.63244452  | 1.37406028  | $e(\frac{2}{3})/2 + \delta$ | $0.15012282 + 0.78657327i$  |
| $e(\frac{1}{3})$ | 10.69551431 | 3.18301083  | $e(\frac{2}{3})/2 + \delta$ | $0.62468273 - 0.09470423i$  |
| $e(\frac{1}{3})$ | 11.25849528 | 1.13707825  | $e(\frac{2}{3})/2 + \delta$ | $-0.11242070 + 0.10083473i$ |
| $e(\frac{1}{3})$ | 12.64900811 | 0.92183852  | $e(\frac{2}{3})/2 + \delta$ | $-0.80493907 - 0.12717437i$ |
| $e(\frac{2}{3})$ | 8.95466251  | 2.93659153  | $e(\frac{1}{3})/2 + \delta$ | $0.36025530 - 0.35631998i$  |
| $e(\frac{2}{3})$ | 10.06466234 | 4.51670022  | $e(\frac{1}{3})/2 + \delta$ | $-0.90149321 - 0.57545547i$ |
| $e(\frac{2}{3})$ | 10.73782624 | 2.37415775  | $e(\frac{1}{3})/2 + \delta$ | $-0.53488262 + 0.88247158i$ |
| $e(\frac{2}{3})$ | 10.82653286 | 0.77122693  | $e(\frac{1}{3})/2 + \delta$ | $0.58740526 - 0.33415990i$  |

TABLE 3.2. Spectral parameters  $(\lambda_1, \lambda_2)$ , sign  $(\epsilon)$ , and sample Dirichlet series coefficients for  $L$ -functions of level 4 of degree 3 Maass forms. Here  $e(x) = \exp(2\pi ix)$  and  $|\delta| < 10^{-9}$ . The numbers are truncated to what we believe are 8 correct decimals.

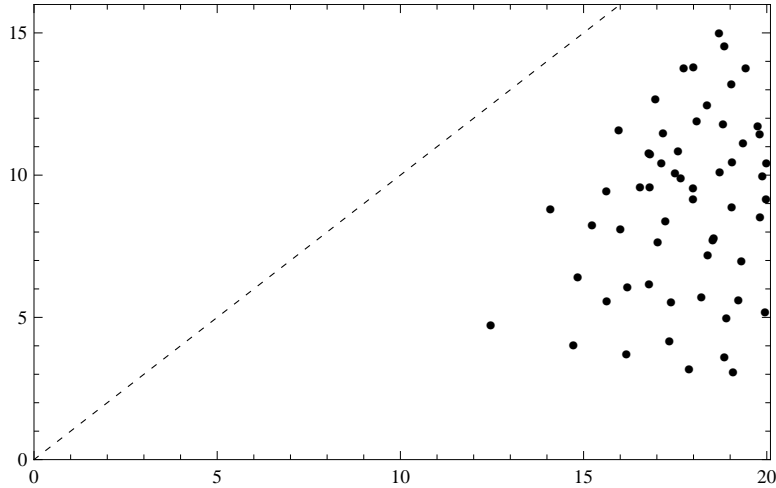


FIGURE 3.2. The axes are  $\lambda_1$  and  $\lambda_2$  and the dots indicate  $(\lambda_1, \lambda_2, -\lambda_1, -\lambda_2)$  for the first few  $Sp(4, \mathbb{Z})$   $L$ -functions. Note that we may assume  $\lambda_1 \geq \lambda_2$ .

We have also found more than 200  $L$ -functions of  $SL(4, \mathbb{Z})$  Maass forms that are not  $Sp(4, \mathbb{Z})$   $L$ -functions. We list the eigenvalues and first few coefficients of the smallest example. We believe that all the given digits are correct:

$$\begin{aligned}
 (\lambda_1, \lambda_2, \lambda_3) &= (13.048202385582, 6.726210585782, -4.367763225255) \\
 a_2 &= -0.1912480688849 - 0.587500805369i \\
 a_3 &= -0.652904479858 + 0.96315195085i \\
 a_4 &= -0.5309393169 + 0.22471678899i \\
 a_5 &= -0.3125111187 - 0.0112785467i.
 \end{aligned}$$

| $\lambda_1$ | $\lambda_2$ | $a_2$       | $a_3$       | $a_5$      | $a_7$     |
|-------------|-------------|-------------|-------------|------------|-----------|
| 12.46875226 | 4.72095103  | 1.34260324  | -0.18745190 | -0.0016279 | 0.228229  |
| 14.09372017 | 8.83036460  | -0.31644276 | 0.05294768  | 0.0261060  | 0.952439  |
| 14.72547970 | 4.02669357  | 0.73680321  | 0.99830784  | 0.2677819  | -0.031085 |
| 14.83756247 | 6.41243964  | 0.18715348  | -0.21546510 | 0.5492948  | 0.582942  |
| 15.23336181 | 8.25653712  | 0.88602292  | 1.76959583  | -0.1217794 | -0.179071 |
| 15.62467181 | 9.46217647  | -1.72583459 | 1.11618173  | -0.6444860 | -0.009432 |
| 15.63453910 | 5.57458793  | 2.30065434  | 0.16113045  | -0.4928333 | -0.410839 |
| 15.96343790 | 11.59606479 | 0.17708238  | -0.36379926 | -1.3728032 | 0.233579  |
| 16.00467179 | 8.12341090  | -0.59748302 | -1.00280803 | -1.5990447 | 0.398796  |
| 16.17300694 | 3.71016260  | 0.60584003  | 0.74786457  | -1.1437477 | 0.469017  |
| 16.19395973 | 6.05889766  | 0.04742685  | 0.01653540  | 1.6223066  | -0.080626 |
| 16.54574513 | 9.57822088  | 0.27348521  | 0.97263132  | 1.4040048  | -0.955692 |
| 16.77928785 | 10.78021484 | -1.50813572 | -0.48797568 | 0.1694122  | -0.471615 |
| 16.78915308 | 6.16376335  | -1.29328034 | -1.51751705 | -0.0818331 | -0.784244 |
| 16.81031209 | 9.58414788  | 0.22614271  | -0.89126171 | 0.0562885  | -0.906897 |

TABLE 3.3. Spectral parameters  $(\lambda_1, \lambda_2)$  and sample Dirichlet series coefficients for 15  $L$ -functions of  $Sp(4, \mathbb{Z})$  Maass forms. The numbers are truncated to what we believe are 8 correct decimals.

Numerical values of the spectral parameters and  $a_2$  for the first 15 examples we found are listed in Table 3.4. They are normalized so that  $\lambda_1 \geq \lambda_2 \geq \lambda_3 \geq \lambda_4$  and  $|\lambda_1| < |\lambda_4|$  and in lexicographical order. We don't claim that this list necessarily contains the first 15  $L$ -functions with this ordering. The full list, including the Dirichlet coefficients, will be made available at <http://www.LMFDB.org/L/degree4>.

**3.6. Other types of degree 4  $L$ -functions.** As a test of the approximate functional equation method, we now apply it to a different type of degree 4  $L$ -function. In this example, we search for  $L$ -functions satisfying a functional equation of the form

$$\Lambda(s) = \Gamma_{\mathbb{C}}(s + \frac{1}{2})\Gamma_{\mathbb{C}}(s + k - \frac{3}{2})L(s) = \Lambda(1 - s). \quad (3.6)$$

That is the functional equation of the spin  $L$ -function of a Siegel modular form of weight  $k$  on  $Sp(4, \mathbb{Z})$ . As a demonstration of the method, let  $k = 20$ . It is known that there is exactly one such  $L$ -function, associated to the cusp form denoted  $\Upsilon_{20}$ . Its first few Dirichlet coefficients, in the arithmetic normalization, are the following rational integers [26]:

$$\begin{aligned} 2^{37/2}a_2 &= -840960 \\ 3^{37/2}a_3 &= 346935960 \\ 4^{37/2}a_4 &= 316975677440 \\ 5^{37/2}a_5 &= -5232247240500. \end{aligned} \quad (3.7)$$

We applied the method of Section 4 to search for the Dirichlet coefficients of an  $L$ -function satisfying the functional equation (3.6) with  $k = 20$ , and having a degree-4 Euler product. We used the first 90 terms of the Dirichlet series, which is 30 unknowns because a degree-4 local factor is determined by  $a_p$  and  $a_{p^2}$ . We chose 30 triples  $(\frac{1}{2} + it, g_1, g_2)$  with  $0 \leq t \leq 33$ ,



| $\lambda_1$ | $\lambda_2$ | $\lambda_3$  | $a_2$                     |
|-------------|-------------|--------------|---------------------------|
| 13.04820238 | 6.72621058  | -4.36776322  | -0.19124806 - 0.58750080i |
| 13.74207582 | 8.91090555  | -6.67116480  | -0.38362321 + 0.88277671i |
| 14.94493797 | 10.17319896 | -7.63795646  | 0.50916811 + 0.08060143i  |
| 15.82354814 | 5.98442035  | -3.32054209  | 0.06707773 - 2.25215645i  |
| 15.84333613 | 8.14020386  | -6.39808715  | -0.93727868 + 0.45045257i |
| 15.94944916 | 11.22357307 | -7.46849155  | -0.01250803 - 0.16785927i |
| 15.99896071 | 5.55250290  | -4.28979199  | 0.76641492 + 0.72684214i  |
| 16.04868870 | 7.44354895  | -5.74749580  | 0.39710090 - 1.01290587i  |
| 16.17564264 | 9.31222108  | -7.99494686  | -0.25094605 - 1.40588826i |
| 16.72584930 | 10.57549478 | -8.05016487  | -1.81300469 - 0.42294306i |
| 16.89972715 | 2.27258771  | -6.03583588  | 0.55659019 + 0.92818484i  |
| 16.92627200 | 12.47850050 | -10.63475738 | 0.33041049 + 0.59891916i  |
| 16.95696382 | 9.53674609  | -7.32770475  | -0.66772182 + 0.75485571i |
| 17.16046064 | 5.51936319  | -3.67883841  | -0.31914164 - 0.69706013i |
| 17.27511800 | 7.18638875  | -4.38401627  | -0.13829583 + 1.09540674i |

TABLE 3.4. Spectral parameters  $(\lambda_1, \lambda_2, \lambda_3)$  and  $a_2$  for  $L$ -functions of  $SL(4, \mathbb{Z})$  Maass forms. The numbers are truncated to what we believe are 8 correct decimals.

selected so that the truncation error in eliminating  $a_n$  for  $n > 90$  is less than  $10^{-12}$ . After using the Euler relations to convert to a non-linear system, we solved the system 1000 times using the secant method with random starting values. Only one solution was found (and it was found repeatedly), which had:

$$\begin{aligned}
2^{37/2}a_2 &= -840960.000014382993 \\
3^{37/2}a_3 &= 346935960.202402521 \\
4^{37/2}a_4 &= 316975677305.428055 \\
5^{37/2}a_5 &= -5232247227434.34870.
\end{aligned} \tag{3.8}$$

We see that the (rescaled)  $a_2$  is convincingly close to an integer, and it is the correct integer. Replacing  $a_2$  by its apparent exact value, and the re-solving for the other coefficients, we find:

$$\begin{aligned}
3^{37/2}a_3 &= 346935959.999827467 \\
4^{37/2}a_4 &= 316975677440.106735 \\
5^{37/2}a_5 &= -5232247240497.56648.
\end{aligned} \tag{3.9}$$

Now the rescaled  $a_3$  is convincingly close to an integer, and again it is the correct integer. Replacing  $a_3$  by its apparent exact value, and solving again we find:

$$\begin{aligned}
4^{37/2}a_4 &= 316975677439.993180 \\
5^{37/2}a_5 &= -5232247240498.27543.
\end{aligned} \tag{3.10}$$

This time, the situation is less clear. The rescaled  $a_4$  certainly appears to be close to an integer; in fact the correct integer. But we had truncated the Dirichlet series to give 12 digits of accuracy. Since the true value of  $4^{37/2}a_4$  is an integer with 12 digits, our calculation should

not have been adequate to determine that integer exactly. It is somewhat surprising that we obtain a few more correct digits than we should have expected.

This example illustrates that the approximate functional equation method should be applicable to other types of  $L$ -functions. We will address these extensions of the method in a subsequent paper.

#### 4. THE METHOD: APPROXIMATE FUNCTIONAL EQUATIONS

Our method of locating  $L$ -functions is based on a smoothed approximate functional equation. The approximate functional equation is a tool that typically is used to prove results about  $L$ -functions (such as moments), or to calculate  $L$ -functions [22]. Here we turn it into a method of locating  $L$ -functions by exploiting the fact that the approximate functional equation contains a free parameter. This approach was inspired by Michael Rubinstein's *Lcalc* program [22, 23].

##### 4.1. Smoothed approximate functional equation. Let

$$L(s) = \sum_{n=1}^{\infty} \frac{a_n}{n^s} \quad (4.1)$$

be a Dirichlet series that converges absolutely in a half plane,  $\Re(s) > \sigma_1$ .

Let

$$\Lambda(s) = Q^s \left( \prod_{j=1}^a \Gamma(\kappa_j s + \lambda_j) \right) L(s), \quad (4.2)$$

with  $Q, \kappa_j \in \mathbb{R}^+$ ,  $\Re(\lambda_j) \geq 0$ . Note that the functional equation we present here is somewhat more general than given in the previous section. We assume that:

- (1)  $\Lambda(s)$  has a meromorphic continuation to all of  $\mathbb{C}$  with simple poles at  $s_1, \dots, s_\ell$  and corresponding residues  $r_1, \dots, r_\ell$ .
- (2)  $\Lambda(s) = \varepsilon \overline{\Lambda(1 - \bar{s})}$  for some  $\varepsilon \in \mathbb{C}$ ,  $|\varepsilon| = 1$ .
- (3) For any  $\sigma_2 \leq \sigma_3$ ,  $L(\sigma + it) = O(\exp t^A)$  for some  $A > 0$ , as  $|t| \rightarrow \infty$ ,  $\sigma_2 \leq \sigma \leq \sigma_3$ , with  $A$  and the constant in the 'Oh' notation depending on  $\sigma_2$  and  $\sigma_3$ .

To obtain a smoothed approximate functional equation with desirable properties, Rubinstein [22] introduces an auxiliary function. Let  $g : \mathbb{C} \rightarrow \mathbb{C}$  be an entire function that, for fixed  $s$ , satisfies

$$|\Lambda(z + s)g(z + s)z^{-1}| \rightarrow 0$$

as  $|\Im(z)| \rightarrow \infty$ , in vertical strips,  $-x_0 \leq \Re(z) \leq x_0$ . The smoothed approximate functional equation has the following form.

**Theorem 4.1.** *For  $s \notin \{s_1, \dots, s_\ell\}$ , and  $L(s)$ ,  $g(s)$  as above,*

$$\Lambda(s)g(s) = \sum_{k=1}^{\ell} \frac{r_k g(s_k)}{s - s_k} + Q^s \sum_{n=1}^{\infty} \frac{a_n}{n^s} f_1(s, n) + \varepsilon Q^{1-s} \sum_{n=1}^{\infty} \frac{\overline{a_n}}{n^{1-s}} f_2(1 - s, n) \quad (4.3)$$

where

$$\begin{aligned} f_1(s, n) &:= \frac{1}{2\pi i} \int_{\nu-i\infty}^{\nu+i\infty} \prod_{j=1}^a \Gamma(\kappa_j(z+s) + \lambda_j) z^{-1} g(s+z) (Q/n)^z dz \\ f_2(1-s, n) &:= \frac{1}{2\pi i} \int_{\nu-i\infty}^{\nu+i\infty} \prod_{j=1}^a \Gamma(\kappa_j(z+1-s) + \bar{\lambda}_j) z^{-1} g(s-z) (Q/n)^z dz \end{aligned} \quad (4.4)$$

with  $\nu > \max\{0, -\Re(\lambda_1/\kappa_1 + s), \dots, -\Re(\lambda_a/\kappa_a + s)\}$ .

Note that, despite its name, the approximate functional equation is an exact formula for the  $L$ -function throughout the complex plane.

We assume  $L(s)$  continues to an entire function, so the first sum in (4.3) does not appear. For fixed  $Q, \kappa, \lambda, \varepsilon$ , sequence  $\{a_n\}$ , and function  $g(s)$ , the right side of (4.3) can be evaluated to high precision. In the next section we describe how we use this observation to model the functional equation.

**4.2. Modeling the functional equation.** The Z-function (or Hardy Z-function) of an  $L$ -function is an analytic function which is smooth and real on the  $\frac{1}{2}$ -line and satisfies  $|Z(\frac{1}{2} + it)| = |L(\frac{1}{2} + it)|$  for  $t \in \mathbb{R}$ . In terms of the completed  $L$ -function (4.2),

$$Z(\tfrac{1}{2} + it) = (\varepsilon Q)^{-\frac{1}{2}} \prod_{j=1}^a |\Gamma(\kappa_j(\tfrac{1}{2} + it) + \lambda_j)|^{-1} \cdot \Lambda(\tfrac{1}{2} + it), \quad (4.5)$$

when  $t \in \mathbb{R}$ . That formula is not a valid definition of  $Z(\frac{1}{2} + it)$  if  $t \notin \mathbb{R}$ , but it is sufficient for our purposes because we will only evaluate the  $L$ -function on the critical line. We will find the Z-function to be convenient because all calculations will involve real numbers instead of complex numbers.

Fix all the parameters in the functional equation of an  $L$ -function and write (4.3) as  $\Lambda(s)g(s) = \text{AppFE}(s, Q, \kappa, \lambda, \varepsilon, \{a_n\}, g)$ , where we suppress the contribution of the poles because we will assume our  $L$ -functions are entire. Use (4.5) to rewrite (4.3) as

$$\begin{aligned} Z(s) = Z(s, g) &= g(s)^{-1} (\varepsilon Q)^{\frac{1}{2}} \prod_{j=1}^a |\Gamma(\kappa_j s + \lambda_j)|^{-1} \text{AppFE}(s, Q, \kappa, \lambda, \varepsilon, \{a_n\}, g) \\ &= g(s)^{-1} \text{RHS}(s, Q, \kappa, \lambda, \varepsilon, \{a_n\}, g), \end{aligned} \quad (4.6)$$

say.

The only free parameters in the above equation are the complex number  $s$  and the function  $g$ . The left side of (4.6) does not depend on the function  $g$ . Thus, for each fixed  $s$ , if we evaluate the right side of (4.6) with two different  $g$  functions  $g_1, g_2$ , then setting them equal gives an equation in the Dirichlet coefficients of the  $L$ -function.

Thus, if we fix  $s_0 = \frac{1}{2} + it_0$  and choose two functions  $g_1, g_2$  then

$$g_1(s_0)^{-1} \text{RHS}(s_0, Q, \kappa, \lambda, \varepsilon, \{a_n\}, g_1) - g_2(s_0)^{-1} \text{RHS}(s_0, Q, \kappa, \lambda, \varepsilon, \{a_n\}, g_2) = 0 \quad (4.7)$$

is a linear equation which the Dirichlet coefficients of the  $L$ -function must satisfy.

We can produce many equations by choosing various  $(s, g_1, g_2)$  combinations. If we have chosen functional equation parameters which correspond to a genuine  $L$ -function, then its Dirichlet coefficients will be a solution to that system. If we have chosen parameters for which

there is no  $L$ -function, then it may be possible to detect this through an inconsistency in the system.

We expand on this approach in the next section.

**4.3. The method.** It is easiest to first think of the functional equation as given, and focus on determining the Dirichlet coefficients. For the case of Maass forms, we do not actually know the functional equation in advance: we must find the spectral parameters  $\lambda_1, \dots, \lambda_{d-1}$  which determine the functional equation. This is an added complication which we address in Section 5.1.

Assume we are given the functional equation of an  $L$ -function and we want to find its Dirichlet coefficients. The main idea is to first choose various  $s_j = \frac{1}{2} + it_j$ , and pairs of test functions  $g_{j,1}$  and  $g_{j,2}$  to form the system of linear equations  $\{Z(s_j, g_{j,1}) - Z(s_j, g_{j,2}) = 0\}$ .

**Step 1. Forming the linear system**

Typically we choose  $g(s) = e^{-i\beta s + \alpha s^2}$  with  $\beta, \alpha \in \mathbb{R}$ . This is an allowable test function in the approximate functional equation provided  $\alpha > 0$ , or  $\alpha = 0$  and  $|\beta| < \frac{\pi}{2} \sum \kappa_j$ .

We illustrate the ideas with a numerical example. The example concerns the  $L$ -function of a Maass form on  $SL(3, \mathbb{Z})$ , so in (4.2) we set  $Q = \pi^{-3/2}$ ,  $a = 3$ ,  $\kappa_1 = \kappa_2 = \kappa_3 = \frac{1}{2}$ , and  $\varepsilon = 1$ . This specifies all the parameters in the functional equation except  $\lambda_j$ . We illustrate below with the test case  $\lambda = (i\lambda_1, i\lambda_2, i\lambda_3) = (8.4i, 14.2i, -22.6i)$ . Those parameters were chosen randomly, so there is no reason to expect that this corresponds to an actual  $L$ -function. In fact, in Section 7 we will prove that there is no  $L$ -function with that functional equation.

Note that we must treat the real and imaginary parts of the Dirichlet coefficients as separate real variables, so we write  $a_n = b_1(n) + ib_2(n)$  with  $b_1(n), b_2(n) \in \mathbb{R}$ .

We apply the procedure described in the previous section. This involves choosing a complex number  $s_0$  and two test functions  $g_1, g_2$ . Choose  $s_0 = \frac{1}{2} + i$ , and let  $g_1(s) = e^{-is/4}$ . A numerical calculation finds,

$$\begin{aligned} g_1(s_0)^{-1} \text{RHS}(s_0, Q, \kappa, \lambda, \varepsilon, \{a_n\}, g_1) = & \quad (4.8) \\ 1.2860 + 7.7907 b_1(2) + 1.9245 b_2(2) + 0.6653 b_1(3) - 1.0163 b_2(3) \\ + 0.03319 b_1(4) - 0.1197 b_2(4) + \dots + 4.17 \cdot 10^{-6} b_1(8) - 2.37 \cdot 10^{-7} b_2(8) + \dots \end{aligned}$$

The terms decrease rapidly: the coefficients of  $b_1(15)$  and  $b_2(15)$  are less than  $2 \cdot 10^{-13}$ . The exponential decay in the contributions of the Dirichlet coefficients is a general phenomenon [4, 13].

With the same  $s_0$ , now choose  $g_2(s) = e^{-is/2}$ . This gives

$$\begin{aligned} g_2(s_0)^{-1} \text{RHS}(s_0, Q, \kappa, \lambda, \varepsilon, \{a_n\}, g_2) = & \quad (4.9) \\ 2.02524 + 2.2117 b_1(2) + 1.8524 b_2(2) + 0.7408 b_1(3) + 0.2210 b_2(3) \\ + 0.1019 b_1(4) + 0.0922 b_2(4) + \dots + 2.66 \cdot 10^{-6} b_1(8) - 0.0000143 b_2(8) + \dots \end{aligned}$$

Subtracting (4.8) from (4.9), we obtain the following equation which the Dirichlet coefficients of the  $L$ -function must satisfy, *if* such an  $L$ -function exists:

$$\begin{aligned} 0 = 0.7392 - 5.5790 b_1(2) - 0.07216 b_2(2) + 0.07541 b_1(3) + 1.23745 b_2(3) & \quad (4.10) \\ 0.06876 b_1(4) + 0.2119 b_2(4) + \dots - 1.51 \cdot 10^{-6} b_1(8) - 0.0000141 b_2(8) + \dots \end{aligned}$$

We have just found *one* equation which the Dirichlet coefficients of the  $L$ -function (if it exists) must satisfy. The next steps involve truncating the system so that we are dealing with

finitely many unknowns, and choosing various  $(s_0, g_1, g_2)$  combinations to form a system of equations.

**Step 2.** *Truncating the system*

The linear equation from Step 1 has infinitely many unknowns. However, the coefficients of those unknowns decrease rapidly. Thus, once we select a working precision, we can truncate the system with an error less than our working precision.

For the remaining steps, we assume that a working precision,  $\delta$ , has been selected (for example,  $\delta = 10^{-12}$ ), and a given number of Dirichlet coefficients,  $J$ , have been selected (for example,  $J = 30$ , so we need only consider  $a_1, \dots, a_{30}$ ).

**Step 3.** *Choosing the parameters*

Having selected a working precision  $\delta$  and a number of Dirichlet coefficients  $J$ , there are limits to which  $(s, g_1, g_2)$  combinations can be used. Namely, we require that the error in the approximate functional equation be less than  $\delta$  when we use these particular values of  $s$  and  $g_j$  and omit those terms  $a_n$  with  $n > J$ . Note that this requires the Ramanujan bound or some other estimate on the Dirichlet coefficients.

In particular, given  $\delta$  and  $J$ , for each function  $g$ , there is a limited range of  $s$  (which may be empty) which meets the requirement of the chosen truncation error.

In practice, often it is effective to fix  $g_1$  and  $g_2$ , and to vary  $s_j = \frac{1}{2} + it_j$  to obtain different linear equations. However, in order to keep the system of equations as well conditioned as possible, one should aim to have the same rate of convergence in all equations. This can be achieved by varying the functions  $g_1$  and  $g_2$  with the  $s_j$ .

**Step 4.** *Using the Euler product*

Except in some low-degree cases, the linear system will have infinitely many solutions. For example, if there are two  $L$ -functions with the same functional equation, then clearly the linear system will have infinitely many solutions.

In order to get around this, we make use of the Euler product and convert to a non-linear system. The difficulty of working with a non-linear system is partially offset by the fact that the number of unknowns will be much smaller. The Euler product immediately gives that all Dirichlet coefficients are determined by the coefficients at prime powers. Furthermore, for a degree- $d$  Euler product, the local factors are determined by  $[d/2]$  parameters. For example, for degrees 2 and 3, all coefficients are determined by  $a_p$ . And for degrees 4 and 5, all coefficients are determined by  $a_p$  and  $a_{p^2}$ .

We apply the multiplicative relations  $a_6 = a_2a_3$ ,  $a_{12} = a_3a_4$ , etc., to reduce the number of unknowns. Then we apply the recursions arising from the shape of the local factors (for example,  $a_{p^2} = a_p^2 - \bar{a}_p$  in the case of  $SL(3, \mathbb{Z})$  Maass forms) to obtain a system of equations with a minimal number of unknowns. So, for example, for  $SL(3, \mathbb{Z})$  Maass forms the unknowns will be  $\{a_p : p \text{ prime}, p \leq J\}$ .

Note: we refer to the  $a_n$  as the “unknowns,” but in practice we must treat the real and imaginary parts of  $a_n$ , denoted  $b_1(n)$  and  $b_2(n)$ , as separate real unknowns. Since  $a_1 = 1$ , the original linear system has  $2(J - 1)$  real unknowns.

**Step 5.** *Solving the non-linear system*

The non-linear system will have many solutions. Most of these are of no interest and are simply accidental solutions.

We use the secant method to solve the system. This is done repeatedly, typically between 100 and 1000 times, with different starting points. The starting points are always chosen

to have values within the Ramanujan bound since this is supposedly true for the interesting solutions. Typically 0–5 different solutions are found. In most cases, the size of the  $a_n$  in the solutions will grow rapidly with  $n$ . For the accidental solutions, the growth is (almost) as fast as the rate of decrease in the coefficients. For the solutions that are close to approximations of true  $L$ -functions, this is not true. Here the growth in the size of the  $a_n$  is smaller. Thus, the Ramanujan bound is an important ingredient to the method because it allows us to eliminate unwanted solutions. However, there are more efficient ways to avoid extraneous solutions, see Section 5.1.

In practice, it turns out that it is better to begin with not too many unknowns in order to find any of the solutions at all. Once a solution has been found, the number of unknowns may be increased and a new larger system is solved with the previous solution as a starting point. Typically we start with  $10 \leq J \leq 40$  and end with  $60 \leq J \leq 150$ .

The above procedure describes a method for finding the Dirichlet coefficients of an  $L$ -function, given its functional equation and the shape of its Euler product. In the case of Maass form  $L$ -functions, there is the added difficulty of finding the spectral parameters which determine the functional equation. This is discussed in the next section.

## 5. SEARCHING FOR THE SPECTRAL PARAMETERS

When searching for  $L$ -functions of Maass forms on  $SL(d, \mathbb{Z})$  or one of its subgroups, the spectral parameters in the functional equation are not known in advance. The greatest challenge is to find good approximations to these parameters.

**5.1. Initial scan.** The first step is to fix a box in which to initially search for spectral parameters  $\lambda_j$  corresponding to an  $L$ -function. Typically, we use boxes of side length 2, so for  $SL(3, \mathbb{Z})$  and  $Sp(4, \mathbb{Z})$  this will be a square (with side 2), and for  $SL(4, \mathbb{Z})$ , a cube. In this box we make a grid of equally spaced points with a typical step size of  $1/5$  to  $1/25$ .

Next, we choose the number of Dirichlet coefficients,  $J$ , to use and set the working precision (estimated maximal size of truncation error) to  $\delta = 0.5 \cdot 10^{-4}$ . We fix test functions  $g_1$  and  $g_2$  of the form  $g_i(s) = e^{-i\beta_i s + \alpha s^2}$ . After these choices are made, we determine the range  $t \in [T_1, T_2]$  of  $s = \frac{1}{2} + it$  on the critical line for which we have a truncation error less than  $\delta$  in the approximate functional equation. If this range is too small, we increase  $J$  until we achieve a large enough range. Typically the range  $[T_1, T_2]$  will be approximately  $[2 \min\{\lambda_j\}, 2 \max\{\lambda_j\}]$ .

Now we determine the number of unknowns,  $m$ , of the non-linear systems of equations. This will depend on whether we assume the  $L$ -functions are self-dual (meaning that the Dirichlet coefficients are real), and on the degree of the local factors of the Euler product. In the case of  $SL(3, \mathbb{Z})$ ,  $m$  is twice the number of primes less than or equal to  $J$ . For  $Sp(4, \mathbb{Z})$ , it is the number of primes or squares of primes less than or equal to  $J$ . We choose  $m + k$  (typically with  $k = 8$ ) values of  $s_i = \frac{1}{2} + t_i$  in the range  $T_1 < t_j < T_2$ . Of these points,  $m$  of them will be used to make the systems of  $m$  non-linear equations in  $m$  unknowns, and the other  $k$  will be used to detect candidates for first approximations to the spectral parameters, as described in the next subsection.

Now for each point in our grid of spectral parameters  $\lambda_j$ , we go through the following procedure. Since the parameters  $\lambda_j$  and test functions  $g_1$  and  $g_2$  are fixed, each of the points  $s_i$  gives a linear equation of the form (4.7). The Euler product is used to turn these into  $m + k$  non-linear equations with  $m$  unknowns. We choose  $m$  of these equations (same for

all points in the grid) and then use the secant method to solve this non-linear system of equations. The system of equations is solved a fixed number of times (typically 50) with starting points chosen randomly each time. In addition to these random starting points, we also use solutions that have already been found at adjacent points in the grid as additional starting values. Sometimes the system with a given starting point will converge to a solution with given accuracy within a set number of steps and sometimes it will not. For some points in the grid it will converge every time and for some never. These solutions are considered “the same” if the first few coefficients agree to a certain accuracy. So finally we will have a number (typically 0–5) of different solutions at each points in the grid.

**5.2. Refining the search.** Once we have a number of different solutions for each point in the grid, we can find candidates for the functional equation parameters. This is when the  $k$  extra equations come into play. Suppose the spectral parameters used in the system of equations are close to those of an  $L$ -function and the Dirichlet coefficients of the solution are also close to those of the  $L$ -function. Then those coefficients should also be close to solutions to the  $k$  extra equations. Hence we want to find spectral parameters for which there is a solution that makes the  $k$  extra equations close to consistent. We do this by substituting the solution found at each point into the extra equations, forming “indicators” which should measure how far the point is from a true  $L$ -function. We then interpolate to determine where the indicators approximately vanish.

**5.2.1. Collecting nearby solutions.** Since there may be several solutions at each point, some of which may be extraneous, we first collect those solutions which are likely to correspond to the same  $L$ -function.

Fix a point  $P$  in the grid and choose  $D$  adjacent points in the grid where  $D$  is the dimension of the grid. In the case of  $SL(3, \mathbb{Z})$ , we have  $D = 2$  and choose the points just above and just to the right of  $P$ . For each of the solutions at  $P$  we identify the solutions at the adjacent points that are closest. Here ‘closest’ in the sense that the first few coefficients differ by as little as possible. Now we have sets of related solutions at  $D + 1$  adjacent points, and each set could potentially correspond to an  $L$ -function.

**5.2.2. Comparing nearby solutions.** Now we use each set of solutions and the  $k$  extra equations to form indicators, and then interpolate to determine where those indicators (approximately) vanish.

Choose  $D$  of the  $k$  extra equations at each of the  $D + 1$  points. Substitute the related solutions of a set into the  $D$  extra equations to get  $D$  complex numbers (indicators) at each of the  $D + 1$  points. Using linear interpolation we find a point where the indicators are approximately 0, which gives us a candidate for an  $L$ -function. This is done for each of the  $\binom{k}{D}$  choices of extra equations, so we get  $\binom{k}{D}$  candidates. If a large enough proportion (50%) of these candidates is close enough to  $P$  this is considered a good candidate. We evaluate the average (of the central 50%) of these candidates and consider this to be an initial candidate for the spectral parameters of an  $L$ -function, which is passed on the the next step of the process. We also save an interpolation of the first few Dirichlet coefficients of the solutions in the set. These coefficients will serve as a starting point when trying to improve the precision of this candidate.

This process is repeated for each of the related sets of solutions at  $P$  and then for each of the points in the grid. The result of this process is a list of initial candidates for spectral parameters of  $L$ -functions with a first approximation of its Dirichlet coefficients.

**5.3. Zooming in on a candidate.** The final step is to try, for each of the initial candidates, to zoom in to a good approximation for the spectral parameters. This is done in steps where the number of coefficients is gradually increased and hence also the size of the truncation error decreased. Each of these steps is similar to the linear interpolation that gave the initial candidate. A system is created and solved at  $D+1$  adjacent points with the approximation of the Dirichlet coefficients as a starting point. If there are solutions at each of the points, then we get  $\binom{k}{D}$  new approximations in the same way as before. If there is no solution or if the average of the new approximations is far from the first then we stop pursuing that possible  $L$ -function, otherwise we continue. This is repeated with increasingly smaller steps and more coefficients. This process is deemed a success when the maximum difference among the  $\binom{k}{D}$  approximations is less than a given bound (we typically require 8 correct decimals). The average (of the central 50%) of these approximations is saved as a highly probable candidate for spectral parameters of an  $L$ -function.

In practice, this process converges very quickly, typically yielding one or two additional decimal digits in each step. We have implemented the above procedure in Mathematica and will make our data available online [17].

## 6. CHECKS ON THE RESULTS

In this section, we discuss some independent checks which support the claim that our procedure finds approximations to  $L$ -functions of Maass forms.

**6.1. Functional equation for twists.** Bian [2] computed the first four examples of  $L$ -functions of Maass forms for  $SL(3, \mathbb{Z})$ . His method uses a similar starting point, but he also uses the functional equation of many twists of the  $L$ -function. This has the drawback of requiring a large number of coefficients. Already for the first few examples, his method requires a linear system of equations with up to 10000 unknowns. Our search found his four examples and a comparison of spectral parameters and Dirichlet coefficients finds agreement to within the claimed precision. Our method gives a higher precision in the spectral parameters and the first few coefficients, but Bian's method produces more coefficients. Finally, Bian has verified the first 50  $SL(3, \mathbb{Z})$   $L$ -functions found in our search.

**6.2. Properties of the coefficients.** Another check is that in our method we leave  $a_{32}$  (and also  $a_{64}$ ) as unknowns. Hence we obtain a computed value of  $a_{32}$  that we can compare with the value derived from the computed value of  $a_2$ . For all our examples for  $SL(3, \mathbb{Z})$  these values agree to at least three decimal places and in some cases (with larger spectral parameter requiring more coefficients) to as many as eight decimal places. This also gives an independent estimate for the accuracy of the coefficients, which compares well with our estimate based on differences in the approximations in the computation.

A strong check involving the coefficients is that the local factors at the primes dividing the level for  $GL(3)$   $L$ -functions agree to high precision with the predicted value. This is discussed in Section 3.4.

**6.3. Lifts.** A check which we consider to be particularly strong is the analytic continuation and functional equation for higher degree lifts of our  $L$ -functions.

For various  $GL(3)$  examples, we computed the symmetric square of the  $L$ -functions, which has degree 6. That is, we used the functional equation and Dirichlet coefficients of the degree 3  $L$ -function to determine the functional equation and Dirichlet coefficients of



the degree 6  $L$ -function. We then used the method in Theorem 4.2 of [13] to verify that the  $L$ -function satisfies the conjectured functional equation. In all cases we find that degree 6  $L$ -function satisfies the expected functional equation.

For the  $GL(4)$   $L$ -functions, the symmetric square has degree 10. Such high degree  $L$ -functions require a large number of coefficients to be computed accurately, so we were not able to obtain convincing results using the symmetric square. But for the specific case of  $Sp(4, \mathbb{Z})$  there is another option. We claim that we have found the spin  $L$ -functions associated to Maass forms on  $Sp(4, \mathbb{Z})$ . If that is true, then we can use the functional equation data and Dirichlet coefficients to compute the standard  $L$ -function, which has degree 5. (That the standard  $L$ -function can be reconstructed from the spin  $L$ -function can be seen from an examination of the explicit representations given in [13].) We computed the degree 5  $L$ -functions in several cases and found that they satisfy the expected functional equation to high accuracy. We consider this to be a strong confirmation of the legitimacy of our calculations. Numerical data will be made available at <http://www.LMFDB.org/L/degree5>.

### 7. PROOF OF THEOREM 3.1

In this section we describe the proof that the lighter shaded region in Figure 3.1 contains no degree 3  $L$ -functions. The idea of the proof is to use the approximate functional equation method of Section 4 to form a system of linear equations in the Dirichlet coefficients, and then verify that the solution to that system violates the Ramanujan bound, when  $(\lambda_1, \lambda_2)$  are in the shaded region.

We will write out the details for the point  $(\lambda_1, \lambda_2) = (8.4, 14.2)$ . Note that this point is in our shaded region, but it is not in the region excluded by Miller's [20] argument using the explicit formula.

In (4.10) we used the point  $(\lambda_1, \lambda_2) = (8.4, 14.2)$  to form one equation for the coefficients. Now we will make another equation. Choosing  $g_3(s) = e^{is/4}$ , and continuing to use  $s_0 = \frac{1}{2} + i$ , we find

$$\begin{aligned}
 g_3(s_0)^{-1} \text{RHS}(s_0, Q, \kappa, \lambda, \varepsilon, \{a_n\}, g_3) = & \tag{7.1} \\
 & - 1078.21 - 2.38608 b_1(2) - 256.449 b_2(2) - 3.595 b_1(3) + 17.503 b_2(3) \\
 & + 1.0549 b_1(4) - 0.1226 b_2(4) + \dots - 4.84 \cdot 10^{-6} b_1(8) + 0.000012 b_2(8) + \dots
 \end{aligned}$$

Recall that  $a(n)$  are the Dirichlet coefficients, and we write  $a(n) = b_1(n) + ib_2(n)$  with  $b_1, b_2 \in \mathbb{R}$ .

Since (4.8), (4.9), and (7.1) each equal  $Z(\frac{1}{2} + i)$ , setting them all equal gives two linear equations in the Dirichlet coefficients. We can solve for  $b_1(2)$  and  $b_2(2)$  to obtain

$$\begin{aligned}
 b_1(2) = & 0.1866 + 0.0137 b_1(3) + 0.2209 b_2(3) + 0.0122 b_1(4) + 0.0380 b_2(4) + \dots \\
 & - 2.7 \cdot 10^{-7} b_1(8) - 2.5 \cdot 10^{-6} b_2(8) + \dots - 2.3 \cdot 10^{-13} b_1(14) - 1.6 \cdot 10^{-12} b_2(14) \dots \\
 b_2(2) = & - 4.1854 - 0.0170 b_1(3) + 0.0629 b_2(3) + 0.0034 b_1(4) - 0.0015 b_2(4) + \dots \\
 & - 2.4 \cdot 10^{-8} b_1(8) + 1.4 \cdot 10^{-7} b_2(8) + \dots - 1.3 \cdot 10^{-14} b_1(14) + 6.1 \cdot 10^{-14} b_2(14) \dots
 \end{aligned}
 \tag{7.2}$$

Now we impose the Ramanujan bound (3.4) on all the coefficients on the right side of the above equation, giving

$$\begin{aligned} b_1(2) &= 0.1866 \pm 1.33 \\ b_2(2) &= -4.1854 \pm 0.301. \end{aligned} \tag{7.3}$$

Note that the  $\pm$  terms are rigorous bounds, not error estimates. Therefore  $b_2(2) < -3.8842$ , provided all the other Dirichlet coefficients satisfy the Ramanujan bound. Since the Ramanujan bound  $|a(2)| \leq 3$  implies  $|b_2(2)| \leq 3$ , we have a contradiction. The conclusion is that if  $(\lambda_1, \lambda_2)$  are the parameters in the  $\Gamma$ -factors of an  $L$ -function, then not all the Dirichlet coefficients satisfy the Ramanujan bound. Thus, assuming the Ramanujan bound, there is no  $L$ -function with  $(\lambda_1, \lambda_2) = (8.4, 14.2)$ .

We eliminated  $(\lambda_1, \lambda_2) = (8.4, 14.2)$  by solving only two linear equations. Identical calculations over a closely spaced grid of points give the shaded region in Figure 3.1. This proves Theorem 3.1.

It is possible to eliminate a larger region by solving a larger system, but we have not attempted to explore the limit of this method.

#### REFERENCES

- [1] Ce Bian, thesis, University of Bristol, 2009.
- [2] Ce Bian, Computing  $GL(3)$  automorphic forms. *Bull. Lond. Math. Soc.*, 42(5):827–842, 2010.
- [3] Jonathan Bober, J. Brian Conrey, David W. Farmer, Akio Fujii, Sally Koutsoliotas, Stefan Lemurell, Michael Rubinstein, and Hiroyuki Yoshida, The highest lowest zero of general  $L$ -functions, preprint.
- [4] Andrew R. Booker, Artins conjecture, Turings method, and the Riemann hypothesis. *Experiment. Math.*, 15(4):385407, 2006.
- [5] Andrew R. Booker, Andreas Strömbergsson, and Akshay Venkatesh, Effective computation of Maass cusp forms. *Int. Math. Res. Not.* 2006, Art. ID 71281, 34 pp.
- [6] Bump, Daniel, *Automorphic forms on  $GL(3, \mathbf{R})$* . Lecture Notes in Mathematics, 1083. Springer-Verlag, Berlin, 1984. xi+184 pp
- [7] J. Cogdell and I.I. Piatetski-Shapiro, Converse theorems for  $GL(n)$ , *Publ. Math. IHES* 79 (1994), 157–214.
- [8] J. Cogdell and I.I. Piatetski-Shapiro, Converse theorems for  $GL(n)$ , II, *J. Reine Angew. Math.* 507 (1999), 165–188.
- [9] J. B. Conrey, and D. W. Farmer, An extension of Hecke’s converse theorem. *Internat. Math. Res. Notices* 1995, no. 9, 445463.
- [10] D. W. Farmer, S. Koutsoliotas, and S. Lemurell, Modular forms and  $L$ -functions with a partial Euler product, *J. Ramanujan Math Soc.*, vol 23 no 2, 2008.
- [11] D. W. Farmer, S. Koutsoliotas, and S. Lemurell, *in progress*.
- [12] D. W. Farmer and S. Lemurell, Maass forms and their  $L$ -functions. preprint, ArXiv: math.NT/0506102
- [13] David W. Farmer, Nathan C. Ryan, and Ralf Schmidt, Testing the functional equations of a high-degree Euler product. *Pacific J. Math.* 253 (2011), no. 2, 349–366. Preprint available at ArXiv: 1011.1307.
- [14] D. Goldfeld, *Automorphic forms and  $L$ -functions for the group  $GL(n, \mathbf{R})$* . With an appendix by Kevin A. Broughan. Cambridge Studies in Advanced Mathematics, 99. Cambridge University Press, Cambridge, 2006.
- [15] Hejhal, Dennis A. *Eigenvalues of the Laplacian for Hecke triangle groups*. *Mem. Amer. Math. Soc.* 97 (1992), no. 469, vi+165 pp.
- [16] H. Jacquet, I.I. Piatetski-Shapiro, and J. Shalika, Automorphic forms on  $GL(3)$ , I and II, *Ann. Math.* 109 (1979), 169–258.
- [17] The  $L$ -functions and modular forms database, <http://www.LMFDB.org/>.
- [18] Boris Mezhericher, Evaluating Jacquet’s Whittaker functions and Maass forms for  $SL(3, \mathbf{Z})$ , to appear in *Mathematics of Computation*, available at <http://www.math.columbia.edu/~boris/>.

- [19] Stephen D. Miller, A method for computing general automorphic forms on general groups, preprint (2009), ArXiv 0801.3299.
- [20] Stephen D. Miller, On the existence and temperedness of cusp forms for  $SL_3(\mathbb{Z})$ . *J. Reine Angew. Math.* 533 (2001), 127-169.
- [21] Stephen D. Miller, The highest lowest zero and other applications of positivity. *Duke Math. J.* 112 (2002), no. 1, 83-116.
- [22] M. Rubinstein, Computational methods and experiments in analytic number theory, in, "Recent perspectives in random matrix theory and number theory", F.Mezzadri and N.C.Snaith, Eds, LMS 2005.
- [23] *L*, a C++ class library and command line program for computing zeros and values of *L*-functions. Available at <http://www.math.uwaterloo.ca/~mrubinst/>.
- [24] Sage computer algebra system, <http://www.sagemath.org/>.
- [25] A. Selberg, *Old and new results and conjectures about a class of Dirichlet series*, Proceedings of the Amalfi Conference on Analytic Number Theory 1989, Univ. Salerno, Salerno (1992), 367-385.
- [26] Nils-Peter Skoruppa, Computations of Siegel modular forms of genus two. *Math. Comp.* 58 (1992), no. 197, 381-398.
- [27] William A. Stein, An introduction to computing modular forms using modular symbols. in *Algorithmic number theory: lattices, number fields, curves and cryptography*, 641-652, Math. Sci. Res. Inst. Publ., 44, Cambridge Univ. Press, Cambridge, 2008.
- [28] Fredrik Strömberg, Computation of Maass waveforms with nontrivial multiplier systems. *Math. Comp.* 77 (2008), no. 264, 2375-2416.
- [29] N. Templier, *preprint*.
- [30] A. Weil, *Über die Bestimmung Dirichletscher Reihen durch Funktionalgleichungen*, *Math. Ann.* 168 (1967).

AMERICAN INSTITUTE OF MATHEMATICS  
FARMER@AIMATH.ORG

BUCKNELL UNIVERSITY  
KOUTSLTS@BUCKNELL.EDU

CHALMERS UNIVERSITY OF TECHNOLOGY AND  
UNIVERSITY OF GOTHENBURG  
SJ@CHALMERS.SE